IMAGING AND CHARACTERIZATION OF FACIAL STRAIN IN LONG VIDEO SEQUENCES

Matthew A. Shreve, Shaun J. Canavan, Yong Zhang, John R. Sullins, and Rupali Patil

Youngstown State University
Department of Computer Science and Information Systems
Youngstown, OH 44555

ABSTRACT

This paper presents a method for computing strain images of a deformable object in a video sequence. The method includes two steps: in the first step, the motion data between a pair of video frames is generated using a robust optical flow algorithm. In the second step, a strain image is computed by applying a gradient filter to the motion data. The efficacy of the method was demonstrated using 30 video sequences that captured human facial expressions under different lighting conditions. Several key factors and their impact on the quality of strain images were also discussed.

Index Terms— Strain Imaging, Optical Flow, Face Video.

1. INTRODUCTION

Imaging objects' elastic properties based on the observed deformation has a broad range of applications. For example, a large amount of research has been done in elastography for cancer diagnosis in the breast, kidney and heart [1, 2], because diseased tissues are correlated with change of elasticity (stiffness). Measuring tissue elasticity also plays an important role in biomechanical modeling for image registration and surgery planning, because modeling accuracy is dependent upon the material parameters being used [3, 4]. Strain imaging has also found applications in damage detection in composite materials [5]. Recently, dynamic strain images have been used in face recognition and forensic investigations [6].

There are two basic approaches to image elastic properties: (1) Recover the absolute values of elastic moduli by solving an inverse problem; (2) Compute strain from measured displacement (motion) and then use the spatial variation of strain as an indicator of underlying tissue properties. Since an inverse problem is often ill-posed and highly nonlinear, the computational complexity of the first approach is relatively high. Various regularization techniques must be used in order to stabilize an inverse solution [7]. The second approach is essentially a forward problem and therefore can be implemented with conventional image filtering methods.

Modalities that have been used in strain imaging include ultrasonic, magnetic resonance (MR) and optical sensors. Elastograms generated from ultrasonic and MR sensors are suitable for examining property abnormalities of internal organs. However, ultrasonic images are plagued by artifacts while high resolution MR images are more expensive. In addition, the imaging devices are often designed to be operated in a well-controlled clinical environment, which restrict their usage to medical fields only.

In this paper, we propose a strain imaging method that is based on the optical flow technique and the gradient filtering. The proposed method has several advantages:

1. It is efficient and can be used to process large amounts of video in a reasonable time framework. With further optimization, it can also be considered for real time applications.
2. Video data can be acquired using optical camcorders. Strain images derived from those videos are adequate for many applications. The method can be used in both indoor and outdoor settings. For example, it can be used to monitor the structural fatigue and damage of endangered bridges and buildings. It can also be used to test the strength and durability of fabrics and other man-made materials.
3. Because of its non-invasive nature, the proposed method can be applied to areas besides facial strain analysis. For example, it is particularly suited for skin cancer diagnosis and quantitative assessment of burn scars.

2. METHOD

Two solution strategies can be employed to compute strain images. The first is to integrate the strain definition into the formulation of optical flow equations so that strain can be derived directly from the image intensity. This approach skips the intermediate steps and is potentially more efficient. However, computing high order derivatives from original images without appropriate processing could cause numerical difficulties because such a solution is very sensitive to image noise. The second approach is to compute motion and strain separately. This approach is more flexible because it allows us to examine the quality of motion data before they are processed by the strain filters. In this study, we use the second approach.

2.1. Compute Motion Using Optical Flow Method

Optical flow is a well-know motion estimation technique that is based on the brightness conservation principle [8]. Two conditions must be satisfied in order to obtain a reliable solution: (i) the intensity of a point on a moving object remains constant across a pair of frames, and (ii) pixels in a small image window move with a similar velocity. The optical flow equation is often expressed as:

$$(\nabla I)^T \mathbf{p} + I_t = 0, \tag{1}$$

where $I(x, y, t)$ is the image intensity as a spatial and temporal function, x and y are image coordinates and t is time. ∇I and I_t are the spatial and temporal gradients of the intensity function. $\mathbf{p} = [p = \frac{dx}{dt}, q = \frac{dy}{dt}]^T$ denotes horizontal motion and vertical motion.

To ensure the high quality of motion data, we experimented with a few different implementation methods as discussed in [9]. We found that the method formulated in a robust estimation framework yielded consistent and reliable results [10]. Therefore, we used this method to generate all motion data for the subsequent strain computation.

2.2. Compute Strain Using Gradient Filters

Considering a deformable object in a two dimensional space, its motion can be described by a displacement vector $\mathbf{u} = [u, v]^T$. Assuming a small motion, a finite strain tensor can be defined as:

$$\varepsilon = \frac{1}{2}[\nabla \mathbf{u} + (\nabla \mathbf{u})^T], \tag{2}$$

or in an expanded form:

$$\varepsilon = \begin{bmatrix} \varepsilon_{xx} = \frac{\partial u}{\partial x} & \varepsilon_{yx} = \frac{1}{2}(\frac{\partial u}{\partial y} + \frac{\partial v}{\partial x}) \\ \varepsilon_{xy} = \frac{1}{2}(\frac{\partial v}{\partial x} + \frac{\partial u}{\partial y}) & \varepsilon_{yy} = \frac{\partial v}{\partial y} \end{bmatrix}, \tag{3}$$

where (ε_{xx}, ε_{yy}) are normal strain components and (ε_{xy}, ε_{yx}) are shear strain components.

Since strain is defined with respect to the displacement vector (u, v) in a continuous space, we make the following approximation in order to estimate strain from the discrete optical flow data (p, q):

$$p = \frac{dx}{dt} \doteq \frac{\triangle x}{\triangle t} = \frac{u}{\triangle t}, \qquad u = p\triangle t, \tag{4}$$

where $\triangle t$ is the elapsed time between two image frames.

If we compute optical flow and strain using a fixed frame interval throughout a particular video sequence, we can treat $\triangle t$ as a constant and estimate the partial derivatives as follow:

$$\frac{\partial u}{\partial x} = \frac{\partial p}{\partial x}\triangle t, \qquad \frac{\partial u}{\partial y} = \frac{\partial p}{\partial y}\triangle t, \tag{5}$$

$$\frac{\partial v}{\partial x} = \frac{\partial q}{\partial x}\triangle t, \qquad \frac{\partial v}{\partial y} = \frac{\partial q}{\partial y}\triangle t. \tag{6}$$

The above computation scheme can be implemented by applying the Sobel filters to the optical flow data:

$$S_x = \begin{bmatrix} -1 & 0 & 1 \\ -2 & 0 & 2 \\ -1 & 0 & 1 \end{bmatrix}, \quad S_y = \begin{bmatrix} 1 & 2 & 1 \\ 0 & 0 & 0 \\ -1 & -2 & -1 \end{bmatrix}, \tag{7}$$

$$\frac{\partial u}{\partial x} \doteq \frac{\partial p}{\partial x}\triangle t = (S_x * p)\triangle t, \tag{8}$$

$$\frac{\partial u}{\partial y} \doteq \frac{\partial p}{\partial y}\triangle t = (S_y * p)\triangle t, \tag{9}$$

$$\frac{\partial v}{\partial x} \doteq \frac{\partial q}{\partial x}\triangle t = (S_x * q)\triangle t, \tag{10}$$

$$\frac{\partial v}{\partial y} \doteq \frac{\partial q}{\partial y}\triangle t = (S_y * q)\triangle t, \tag{11}$$

where (S_x, S_y) are the Sobel filters and $*$ is the convolution operator.

Given $(\frac{\partial u}{\partial x}, \frac{\partial u}{\partial y}, \frac{\partial v}{\partial x}, \frac{\partial v}{\partial y})$, we can obtain strain components $(\varepsilon_{xx}, \varepsilon_{yy}, \varepsilon_{xy}, \varepsilon_{yx})$ by the definition of (3).

Under the uniform stress, large strain values correspond to low elastic moduli and vice versa. Therefore, elastograms based on the absolute strain value or relative strain ratio can be used to reveal underlying elastic property changes [2]. For this purpose, we compute a strain magnitude as follow:

$$\varepsilon_m = \sqrt{\varepsilon_{xx}^2 + \varepsilon_{xy}^2 + \varepsilon_{yx}^2 + \varepsilon_{yy}^2}. \tag{12}$$

All strain values can then be visualized as images or be further processed for a specific application.

3. EXPERIMENTAL RESULTS

3.1. Data Set

Videos used in this study came from a database that contains videos of over 100 subjects. Each subject was asked to show various facial expressions. Videos were acquired using a Cannon XL1S camcorder with a speed of 30 frames per second. Each subject has a video sequence of over 4000 frames with a resolution of 480 x 720 pixels. Sequences of 30 subjects randomly selected from the database were used in this experiment. Two lighting conditions were considered: regular light and shadow. Figure 1 shows a few sample frames.

3.2. Strain Images

Strain values vary over a wide range, from negative to positive, which make it difficult to visualize. We took the absolute values of each strain component and normalized them to a scale of 0-255 grey levels. Figure 2 shows a typical strain magnitude image obtained using two frames (1142 and 1144) that were extracted from a sequence in which the subject gradually opened his mouth.

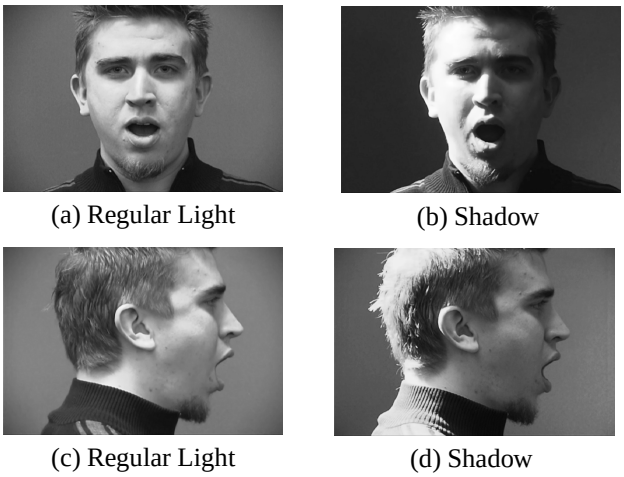

(a) Regular Light (b) Shadow

(c) Regular Light (d) Shadow

Fig. 1. Videos acquired under different lighting conditions.

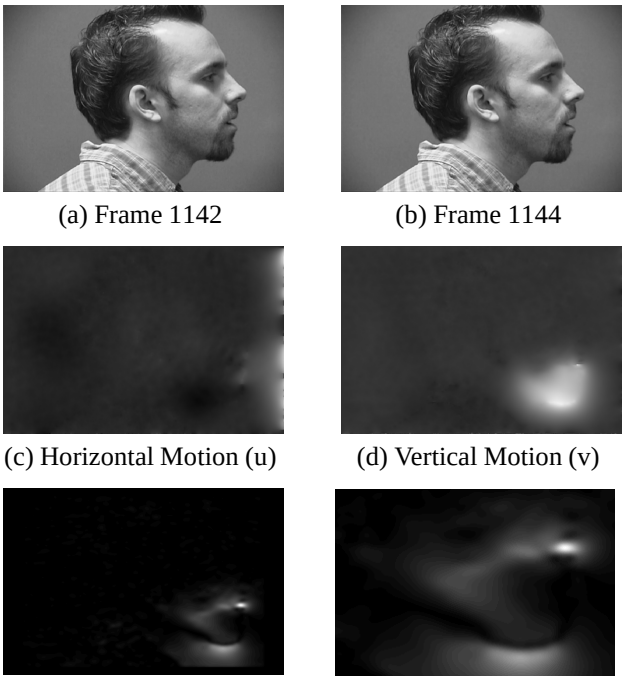

(a) Frame 1142 (b) Frame 1144

(c) Horizontal Motion (u) (d) Vertical Motion (v)

(e) Strain Magnitude (f) Zoomed-in view

Fig. 2. Examples of optical flow and strain images.

Motion between the two frames occurred mainly in the lower portion of the face, which was clearly captured in (Figure 2 (d)), while the horizontal motion was almost negligible. Note that the bright pixels along the right boundary in Figure 2 (c) are noise and were not used in strain computation. As a result, the lower portion of the face has large strain values, while the background has small random strain values only (Figure 2 (e)). As can be seen in the zoomed-in view (Figure 2 (f)), strain distribution of skin is smooth and continuous, a characteristic of deformed soft tissues.

On the other hand, strain discontinuities were observed along the lips and the jaw line. We call this type of strain *pseudo strain*, because it has no connection with true elasticity. Instead, it is caused by the brightness contrast between the background and a moving object. The *pseudo strain* can also be observed when a subject suddenly shakes his/her head or blinks his/her eyes.

4. DISCUSSIONS

The quality of a strain image can be affected by many factors, including those commonly encountered in imaging problems. We discuss two key factors by means of both visual examination and quantitative measures.

4.1. Frame Interval

Because of the small motion constraint imposed on the optical flow equation, the interval between two frames has a strong impact on the quality of motion data, which in turn will effect the quality of strain images.

Figure 3 shows three strain magnitude images using frame pairs of increasing intervals. As expected, strain deteriorated rapidly as the interval increased, and eventually became meaningless when the interval was greater than 5. To provide more quantitative descriptions, we computed a strain difference (SD) between two images that have interval m and interval n:

$$SD = \sum_{i=0}^{ROI} (S_{int=m}(i) - S_{int=n}(i))^2, \qquad (13)$$

where ROI is a selected region of interest and S represents a strain component.

Since a frame interval of 2 usually yields good strain results, we took a strain image (interval = 2) as the base image, and then computed the differences between the base image and a series of strain images with intervals from 1 to 8. The results were plotted in Figure 4. It is clear that all strain components show marked deviation from the base image. It should be pointed out that frame interval is closely related to the video capture speed, and therefore an *optimal* interval is really task-dependent.

4.2. Lighting Condition

It is interesting to notice that lighting conditions do not cause significant deterioration of strain quality, even when severe shadows are present as shown in Figure 5 (b). The overall facial strain pattern was preserved except in a few areas that have strong light reflections caused by hair, beard, earrings, or eye glasses. This may be partially explained by the fact that strain (and optical flow) is more dependent upon the relative change of intensity between two frames than the absolute intensity values.

(a) Frame 1516

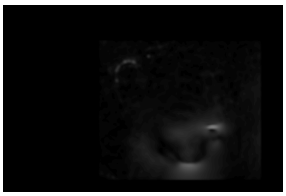

(b) Strain Using Frame-1516 and Frame-1518

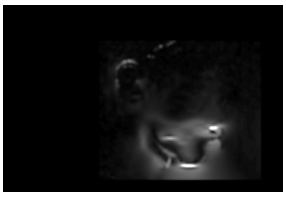

(c) Strain Using Frame-1516 and Frame-1520

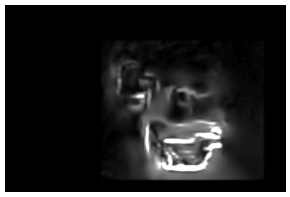

(d) Strain Using Frame-1516 and Frame-1524

Fig. 3. The effect of frame interval on strain images.

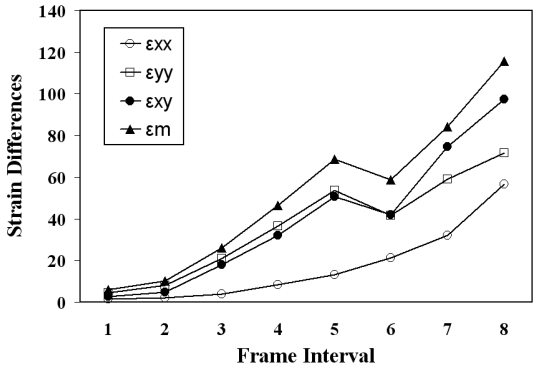

Fig. 4. Strain differences between the base image (interval = 2) and other strain images (interval = 1, 2, ..., 8).

5. SUMMARY

In this paper, we introduced a method for computing strain images of deformable objects in a video sequence. The method employs a two-step approach that combines an optical flow algorithm and a gradient filtering method. The two steps can be carried out separately so that the quality of strain images can be ensured by analyzing the motion data. Promising results were obtained using face video sequences of 30 subjects. We also identified a few key factors and discussed their potential impact on strain images. Although the method was demonstrated using face videos only, it can be applied to a variety of areas, such as skin cancer diagnosis, face biometrics and realistic animation.

6. REFERENCES

[1] J. Bishop A. Samani and D. B. Plewes, "A constrained modulus reconstruction technique for breast cancer assessment," *IEEE Transactions on Med. Imag.*, vol. 20, pp. 877–885, 2001.

[2] J. D'hooge E.E. Konofagou and J. Ophir, "Myocardial elastography - a feasibility study," *Ultrasound in Medicine and Biology*, vol. 28, pp. 475–482, 2002.

[3] F. I. Parke and K. Waters, *Computer Facial Animation*, A.K. Peters, Wellesley, Massachusetts, 1997.

[4] F. R. Carls D. F. von Buren G. Fankhauser R. M. Koch, M. H. Gross and Y. I. H. Parish, "Simulating facial surgery using finite element models," in *Proceedings of SIGGRAPH*, 1996, pp. 421–428.

[5] M. Johnson M. Kunzler, E. Udd and K. Mildenhall, "Use of multidimensional fiber grating strain sensors for damage detection in composite pressure vessels," in *Proceedings of the SPIE*, 2005, vol. 5758, pp. 83–92.

[6] xxxx xxxx xxxx, xxxx, "Facial strain pattern as a soft forensic evidence," in *Proceedings of WACV-2007*, Austin, Texas, Feb. 2007 (to appear).

[7] F. Kallel and M. Bertrand, "Tissue elasticity reconstruction using linear perturbation method," *IEEE Trans. Medical Imaging*, vol. 15, pp. 299–313, 1996.

[8] B.K.P. Horn and B.G. Schunck, "Determining optical flow," *AI Memo 572. MIT*, 1980.

[9] D. J. Fleet J. L. Barron and S. S. Beauchemin, "Performance of optical flow techniques," *International Journal of Computer Vision*, vol. 12, no. 1, pp. 43–77, 1994.

[10] M. J. Black and P. Anandan, "The robust estimation of multiple motions: Parametric and piecewise-smooth flow fields," *Computer Vision and Image Understanding*, vol. 63, no. 1, pp. 75–104, 1996.

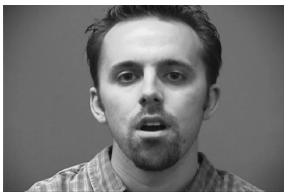

(a) Regular Light

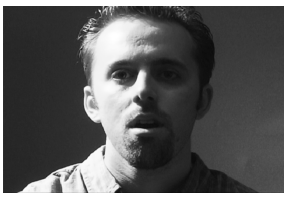

(b) Shadow

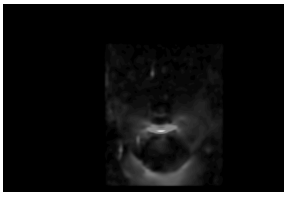

(c) Regular Light Strain

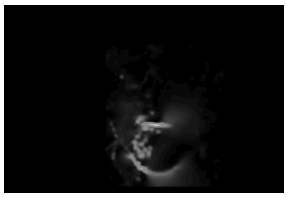

(d) Shadow Strain

Fig. 5. The effect of lighting conditions on strain images.